



Historical contingency in fluviokarst landscape evolution

Jonathan D. Phillips

Tobacco Road Research Team, Department of Geography, University of Kentucky, Lexington, KY 40506-0027, USA

ARTICLE INFO

Article history:

Received 11 September 2017
 Received in revised form 19 November 2017
 Accepted 19 November 2017
 Available online 22 November 2017

Keywords:

Fluviokarst
 Chronosequence
 Landform transitions
 Landscape evolution
 Graph theory

ABSTRACT

Lateral and vertical erosion at meander bends in the Kentucky River gorge area has created a series of strath terraces on the interior of incised meander bends. These represent a chronosequence of fluviokarst landscape evolution from the youngest valley side transition zone near the valley bottom to the oldest upland surface. This five-part chronosequence (not including the active river channel and floodplain) was analyzed in terms of the landforms that occur at each stage or surface. These include dolines, uvalas, karst valleys, pocket valleys, unincised channels, incised channels, and cliffs (smaller features such as swallets and shafts also occur). Landform coincidence analysis shows higher coincidence indices (CI) than would be expected based on an idealized chronosequence. CI values indicate genetic relationships (common causality) among some landforms and unexpected persistence of some features on older surfaces. The idealized and two observed chronosequences were also represented as graphs and analyzed using algebraic graph theory. The two field sites yielded graphs more complex and with less historical contingency than the idealized sequence. Indeed, some of the spectral graph measures for the field sites more closely approximate a purely hypothetical no-historical-contingency benchmark graph. The deviations of observations from the idealized expectations, and the high levels of graph complexity both point to potential transitions among landform types as being the dominant phenomenon, rather than canalization along a particular evolutionary pathway. As the base level of both the fluvial and karst landforms is lowered as the meanders expand, both fluvial and karst denudation are rejuvenated, and landform transitions remain active.

© 2017 Published by Elsevier B.V.

1. Introduction

Landscape evolution can be viewed as a sequence of transitions in landscapes and the landforms that comprise them. While specification of stages may be in some cases an artificial discretization of a continuous process, it is not necessarily misleading to perceive or analyze landscape development in these terms for three reasons. First, given the long time scales of geomorphic evolution relative to human observation, some such simplification is an epistemological necessity. Second, empirical evidence of long-term landscape change is in the form of “snapshots” representing more-or-less distinct stages or episodes (e.g., dated surfaces, space-for-time substitutions, stratigraphic evidence). Finally, many geomorphic changes are threshold-dominated phenomena, such that transitions may indeed be relatively abrupt. In karst, for instance, these include events such as conduit breakthrough, cave or doline collapse, or stream/conduit capture.

This paper investigates the role of historical contingency and canalization in evolution of fluviokarst landscapes in central Kentucky, USA. Here, different stages of development are evident on slip-off slopes of developing meanders of the Kentucky River. The suite of fluvial and karst forms at each stage, and the transitions between stages, are

analyzed in a network context to identify and quantify the historical contingency involved.

1.1. Historical contingency and path dependency

Historical contingency and path dependence are ubiquitous in geomorphology (as well as pedology, ecology, and hydrology). Contingency may involve inheritance of features from earlier periods of formation or sets of environmental controls (legacy effects; for example underfit streams occupying glacially-carved valleys; Dury 1964), conditionality, and dynamical instability. Conditionality occurs when different geomorphic impacts—and potentially different developmental trajectories—are dependent on the occurrence of a particular event, disturbance, or threshold exceedance. Quaternary development of the Kentucky River, for instance, described in Section 2.1 below, is conditional on a Pleistocene ice-damming event in the ancestral Teays River system about 1.5 Ma. Dynamical instability involves landscape “memory” of variations in initial conditions or effects of disturbances due to disproportionate growth and persistence of those effects. Chemical weathering phenomena, including karst dissolution, are often characterized by instability, whereby minor initial differences in resistance due to lithological variations or small structural features become magnified by positive feedbacks (e.g., Twidale 1991; Kauffman 2009). Where historical contingency is present, evolution is path-dependent in that developmental trajectories

E-mail address: jdp@ky.edu.

depend in part on previous states and events, as opposed to convergent evolution toward some state that is historically independent.

Canalization is a form of historical contingency closely related to positive feedbacks and irreversibility. It refers to situations whereby once a particular evolutionary path has been established, other previously possible pathways are eliminated, and evolutionary trajectory is channeled, or canalized. Waddington (1942) coined the term in the context of evolutionary genetics, but it has since been applied more broadly to geophysical and ecological systems (Caloi 1964; Berlow 1997; Levchenko and Starobogatov 1997; Stallins 2006). Several geomorphologists have used the term path dependence to describe canalized landform and landscape evolution (e.g., Naylor and Stephenson 2010; Verleysdonk and Krautblatter 2011; Wainwright et al. 2011; Perron and Fagherrazi 2012). Using an example where the channelization metaphor is literally applicable, whether a channel forms here or a few meters away may be influenced (via dynamical instability) by such tiny variations that it is essentially pseudorandom. Once formed, however, the new channel is a more efficient flow path, and those flows help maintain it and may enlarge it by scour. The formation of the channel was not preordained or deterministically predictable with respect to its precise location, but once established it closes off some previously possible channel locations and strongly influences down-gradient channel locations. Irreversibility can also play a role. Once a portion of a hillslope fails, for example, the slumped material cannot return to its original location. The mass movement and the associated rearrangement of slope morphology influences future slope processes, making some pathways and outcomes more, and others less, likely. Karst landform evolution, in particular, is characterized by important self-reinforcing positive feedbacks between dissolution processes, enlargement of conduits, cavities, and depressions, and hydrologic fluxes (Kauffman 2009).

Historical contingency in Earth and environmental sciences has traditionally been dealt with in three general ways. One involves making it the focus of research, with emphasis on working out histories of landform and landscape evolution and environmental reconstruction. In this approach history is paramount and non-contingent controls are seen as constraining and/or explaining historical sequences. A second is essentially opposite, focusing on non-contingent controls (laws, defined broadly) and viewing historical and geographical contingencies as complications or noise, or details of only local importance. A third general strategy is intermediate, starting with explanation based on non-contingent generalizations, but explicitly addressing place and history factors to elucidate aspects not explained by generally applicable laws. Quantification of historical contingency, consistent with these three approaches, has been based on variance explained by temporal patterns, or residual variation not explained by general principles.

In recent years more explicit approaches to historical contingency have emerged. Beven (2015), focusing on hydrology-ecology-geomorphology interactions, developed a modeling strategy based on event persistence. A conceptually similar field-based approach, particularly important in studies of landform-soil-vegetation coevolution, is focused on the key role of disturbances, and on identifying and measuring effects of disturbances over ecosystem and landscape evolution time scales. Some examples from the forest biogeomorphology literature include Samonil et al. (2009, 2013, 2014). A multi-timescale approach to modeling and analysis can also address historical effects; examples include Sommer et al. (2008) on soil landscape evolution and Vercruyse et al. (2017) on fluvial suspended sediment transport. There has also been a recent explicit emphasis on the role of initial conditions in soil, landform, and ecosystem evolution (Raab et al. 2012; Biber et al. 2013; Maurer and Gerke 2016).

My own contributions have focused on graph theory techniques applied to Earth surface systems represented as networks of interacting components. The graph property of inferential synchronization indicates the extent to which a (geomorphic) system experiences changes contemporaneously or in predictable succession (high

synchronization). Synchronization in the literal sense is not directly applicable to graphs representing historical or evolutionary sequences. However, inferential synchronization is analogous, indicating the extent to which observations or inferences at one point in the network can be applied to components elsewhere in the graph (Phillips 2013). Low synchronization indicates a high degree of historical contingency (and vice versa). Phillips (2012) introduced the graph-based synchronization concept to geomorphology, and Phillips (2013) applied it explicitly (along with other graph-based measures) as a tool for quantifying historical contingency in geomorphic systems.

The related issue of robustness in soil, vegetation, and landform chronosequences was addressed by Phillips (2015a), who adapted stability analysis techniques to measure path stability. Path stability indicates the extent to which developmental trajectories in historical sequences are likely to be repeated if the system is disturbed or the sequence set back to earlier stages. Path instability is associated with high levels of historical contingency. Phillips (2016) depicted evolutionary patterns and sequences as state-and-transition models represented as directed graphs. Several measures of complexity and synchronization were applied to both archetypes of evolutionary sequences, and empirical examples, including soil landscape evolution and river channel morphological changes. This paper applies the methods of Phillips (2013) to a chronosequence represented by the types of landforms present at each stage.

1.2. Fluviokarst landscape evolution

Fluviokarst landscapes are characterized by an interconnected combination of surface and underground hydrological processes and flux paths, and both karst and fluvial landforms. Some landforms may be transitional or hybrid forms. All components of the fluviokarst system are linked to the same base level and regional drainage controls, and thereby coevolve. Both karst-to-fluvial and fluvial-to-karst transitions occur at the scale of individual landforms in the central Kentucky study area (Thrailkill et al. 1991; Phillips et al. 2004; Ray and Blair 2005; Phillips 2017) and in fluviokarst systems in general (e.g., Jaillet et al. 2004; Ortega Becerril et al. 2010; Tiria and Vijulie, 2013; Lipar and Ferk 2015; Woodside and Peterson, 2015).

Early researchers proposed a progression from an initially fluvial landscape to fluviokarst and finally to holokarst (e.g., Cvijic 1918; Roglic 1964). However, it was soon recognized that this progression is not inevitable, and is potentially reversible (e.g., Sawicki 1909; Ford 2007; White 2009), though Bocic et al. (2015) found that landscape evolution of the Una-Korana plateau in the Dinaric karst did approximate the fluvial-to-karst sequence. But in the Monte Berici karst, Italy, for instance, Sauro's (2002) analysis showed that fluvial development is the main morphogenetic process, driven by climate change and tectonic uplift. Later, karst formed on relatively inactive or relict fluvial features. By contrast, in Spain Ortega Becerril et al. (2010) found a switch from domination by dissolutional erosion and karst forms to a prevalence of mechanical erosion and fluvial forms. In yet another variation, some fluviokarst landscapes exhibit divergent evolution into channel-rich, karst-poor and karst-rich, channel-poor zones (e.g., central Kentucky, USA; Phillips et al. 2004; Phillips and Walls 2004). Other areas exhibit sharp contrasts between nearby karst- and fluvially-dominated landscapes, or between karst areas with or without fluvial impacts (e.g., Benac et al. 2013; Bahtjarevic and Faivre 2016).

The interplay of fluvial and karst processes is often conceived, accurately enough, as a “competition” for the excess precipitation that drives both sets of processes. However, at the landscape scale this competition enhances both sets of processes in the central Kentucky study sites studied by Phillips (2017). Evolution of this fluviokarst is best understood as mutual reinforcement, whereby karstification is enhanced by stream incision, and fluvial dissection is often intensified by presence of karst features. This questions the extent to which canalization and historically contingent lock-in are present.

2. Study area and methods

2.1. Study area

The study area is in the valley of the Kentucky River of central Kentucky, focused on the interior area of incised meander bends (Fig. 1). This is in the Inner and Outer Bluegrass physiographic regions, which features a humid subtropical climate, with mean annual precipitation of 1100 to 1200 mm, spread relatively evenly throughout the year. The geological setting is characterized by horizontally bedded Ordovician limestones, with small amounts of dolomite, calcitic shale, and bentonite. The Lexington Limestone formation comprises the unincised upland surfaces. The area has not been tectonically active during the Quaternary, though older faults are found throughout the region. The Inner Bluegrass is dominated by carbonate rocks, mainly limestone, with some thin interbeds of calcareous shales and siltstones. The Outer Bluegrass is also mainly limestone, but with an increased proportion of acidic, non carbonate rocks, particularly shales. The Inner and Outer Bluegrass river reaches shown in Fig. 1 also differ in that the Outer Bluegrass section is more strongly fluvially dissected and less karst-dominated.

Higher-elevation portions of the meander bend interiors studied here lie on the lower part of the Lexington Limestone formation (Grier member). According to the geological map description, this is a light-gray, bioclastic, poorly sorted, fossiliferous limestone in irregular beds about 15 cm thick alternating with sets of nodularly bedded fossiliferous limestone with much micrograined calcite matrix. Lower, eroded portions expose the Tyrone Limestone and Oregon formation, and the Camp Nelson formation. The Tyrone limestone is cryptograined with some clear calcite, or micrograined calcareous dolomite. The Oregon formation is interbedded limestone and dolomite. Camp Nelson limestone, exposed on lower slopes above Quaternary alluvium, is cryptograined limestone with calcareous dolomite (Cressman and Hrabar 1970). All these formations are horizontally bedded, with irregularly spaced vertical and sub-vertical joints.

The Kentucky River, an Ohio River tributary, is the base level for both karst and fluvial systems in the Inner Bluegrass. About 1.3 to 1.8 Ma the river began incising in response to glacial rearrangement of the ancestral Teays River system to which the Kentucky River drained (Teller and Goldthwait 1991; Andrews 2004). This rearrangement resulted in

the displacement of the Teays to the approximate modern alignment of the Ohio River, resulting in a shorter path and steeper slope for the Kentucky and other tributaries to the unglaciated south. The Kentucky River has incised 60 to 130 m since that time, carving the Kentucky River gorge. Tributaries are incising in response, and larger streams have a strongly incised lower reach graded to the Kentucky River (typically with structurally-controlled knickpoints). Smaller tributaries where incision cannot keep pace with the Kentucky River may have hanging valley morphology (Phillips and Lutz 2008). In the larger streams the incision has not reached the upper portions, which are unincised and include sinking streams and dry karst valleys.

The Kentucky River gorge has strongly incised meanders, with slip-off slopes on the bend interiors, and steep slopes, typically palisade-like cliffs, on the outer bends (the area is sometimes referred to as the Palisades). These meanders have been extending since the Pleistocene incision began, as indicated in some cases by high-level fluvial deposits representing the pre-incision path (Andrews 2004; Phillips 2015b). The bend interior slip-off slopes are occupied by strath terraces. Thus a transect normal to the bend apex represents a chronosequence with respect to landform development from the oldest upland surface uneroded by meander extension, across successively younger strath surfaces, to the active fluvial and alluvial areas of the Kentucky River. This sequence is described in more detail in Section 3.1.

2.2. Data collection

Thirty-three meander bends, including 22 bends previously studied to compare the degree of fluvial incision vs. surface karstification on inner vs. outer bends (Phillips 2015b) were examined using geographical information system (GIS) data obtained from the Kentucky Geological Survey (KGS). The purpose was to identify the key karst and fluvial landforms on the bend interiors. Data layers included shaded relief topography derived from 1.5 m (5 ft) LiDAR-derived digital elevation model (DEM) data; 1:24,000 scale US Geological Survey topographic maps; 'blue-line' streams from the topographic maps and the national hydrographic dataset; 1:24,000 scale geological maps; and karst potential maps at the same scale. The latter are based on lithology, and include categories of very high, high, moderate, and low karst potential, and non-karst. Both true and false-color imagery at horizontal resolutions as fine as 0.3 m (1 ft) was used, with imagery taken between 2006 and 2015. Supporting GIS layers included coverage of springs and water wells. A karst potential map of Kentucky (1:24,000 scale), and coverage of sinkhole outlines were also used. All data (except for some of the true-color aerial photographs, accessed through Google Earth™) were obtained through the Kentucky Geological Survey (KGS; <http://kgs.uky.edu/kgsweb/main.asp#tabs-2>). The Harrodsburg sheet of the Karst Atlas of Kentucky (Currens et al. 2003) was also used. The atlas shows groundwater flow paths determined by dye tracing, mapped karst groundwater basins, springs, and stream sinks.

The 22 bends analyzed in earlier studies (Phillips 2015b) were expanded to include more of the Inner Bluegrass section of the Kentucky River, as the Outer Bluegrass bends are not fully comparable with respect to karstification, given their more variable lithology. The downstream (northwest) limit was established because farther downstream near Frankfort, several Quaternary cutoffs and an avulsion occurred, such that the lateral channel change dynamics have differed from the studied meanders.

Two bends were examined in detail in the field—the western, downstream portion of the compound Polly's Bend, and Bowman's Bend (Fig. 1). These were chosen because both are within Kentucky State Nature Preserves, simplifying access and representing sites where little or no recent modification has occurred due to agriculture, construction, landscaping, or other activities, though upper portions of the bend interiors were logged or grazed in the past (Martin 2006). At these sites the landforms identified from GIS analysis were ground-truthed. The distribution of rounded quartz gravels was also mapped. Because the local

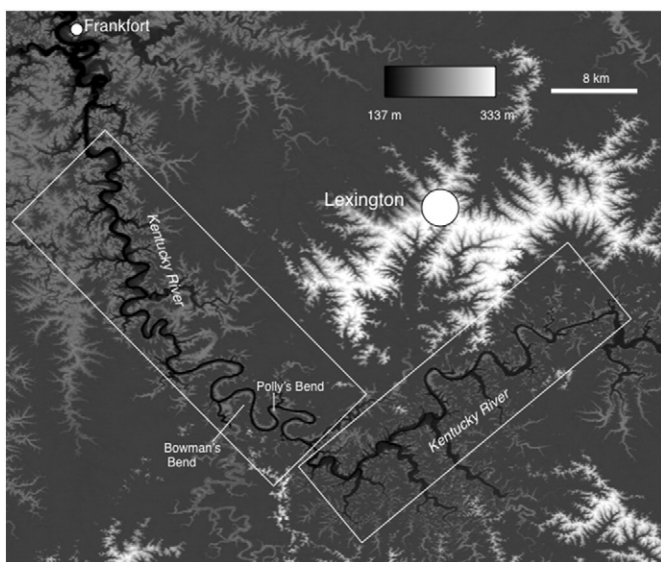


Fig. 1. Elevation density map of study area. Boxed areas includes the 33 meander bends examined via GIS data. The left (downstream) box includes those bends within the Inner Bluegrass physiographic region; the right (upstream) section is in the Outer Bluegrass region.

rock contains no quartz or quartz-bearing sedimentary rocks, these are indicative of material originally deposited by the Kentucky River.

Karst and fluviokarst landforms present on the bend interiors were identified. Not all features are evident from GIS data at all bends, but all are present at Bowman's and Polly's Bend, as well as some others. At the study sites, the landforms were assigned to the chronosequence surfaces.

The terrace surfaces were delineated based on topography, distribution of rounded quartz gravels, and surficial geology. Despite subsequent fluvial and karst erosional modification, some terrace-and-riser morphology is evident at the field sites. The quartz gravels help delineate areas clearly once occupied by the migrating Kentucky River channel, and the exposure of different geological formations is indicative of the beveling off of the bend interiors.

Based on data collection for this study, and published results from previous work in the study region, a proposed model sequence of development of the interior of the incised meander bends of the Kentucky River was developed for comparison with field observations. The previous work includes karst groundwater basin and flowpath mapping by Currens et al. (2003); and studies of karst springs by Ray and Blair (2005). Andrews' (2004) reconstructed the Plio-Pleistocene evolution of the Kentucky River, which incorporates earlier studies of Kentucky River deposits and paleochannels, and Phillips et al. (2004), Phillips and Walls (2004), and Jerin and Phillips (2017) studied fluvial-karst and karst-fluvial transitions. The previous work also includes Martin's (2006) detailed examination of vegetation, hydrological, pedological, and geomorphic interactions at Bowman's Bend, analysis of the contrasting karst and fluvial processes and landforms at inner and outer areas of Kentucky River meanders by Phillips (2015b), and the fluviokarst landscape evolution study of Phillips (2017), which included the Polly's Bend site.

2.3. Graph analysis

The spatial distribution of landforms on a chronosequence can be analyzed via a coincidence matrix and adjacency graph. If two landforms always occur together (coincidence index $CI = 1$) then it can be inferred that they are either genetically related, and/or that both are ubiquitous in the landscape, independently of age or stage. If $CI = 0$ (the landforms never occur together) they are not genetically related and occur at different stages of landscape development. A random pattern of co-occurrence would produce $CI = 0.5$. In this study

$$CI_{a,b} = (\sum q_{a,b})/q \quad (1)$$

where $q_{a,b}$ is a surface or chronosequence member where landforms a,b occur together, and q is the number of chronosequence members.

Simple, undirected graphs were produced for both the idealized and observed cases. The graphs contain $N = q \sum n_q$ nodes, where there are q ($= 5$ in this case) chronosequence stages or surfaces and n_q is the number of landform types at each stage. All nodes (landforms) at each stage are considered to be linked. If the same landform occurs on spatially and temporally adjacent surfaces, then they are also linked.

If the same landform occurs on two adjacent (succeeding) portions of the chrono-sequence, this implies either the landform itself, or the processes by which it is created, persist from the older to the younger stage. The number of links $m = \sum (n_q - 1) + p_c$, where p_c is the number of links representing the same landform on adjacent surfaces. For this study the maximum possible N is 35 (seven landforms, all of which occur on each of the five surfaces), and the maximum possible m is 133.

The graphs were analyzed via metrics from algebraic graph theory, applied to the adjacency matrices of the graphs (in this case, entries are 1 if two nodes are connected and 0 otherwise). The graph spectrum of eigenvalues $\lambda_1, \lambda_2, \dots, \lambda_N$ can be computed from the adjacency matrix. The λ_i have the property $\lambda_1 \geq \lambda_2 \geq \dots \geq \lambda_N$. The largest eigenvalue (λ_1) is called the spectral radius, and is a standard measure of graph complexity.

The spectral radius is particularly sensitive to the number of loops (sequences of linked nodes that start and end at the same node). λ_1 is highest for a graph where every node is connected to every other ($\lambda_1 = N - 1$ for that case). For a given N, m the maximum largest eigenvalue is

$$\lambda_{max} = [2m(N-1)/N]^{0.5} \quad (2)$$

The relative importance (ζ) of the number of connections (edges) in a graph and the specific network of connections ("wiring") to the spectral radius can be determined by (Phillips 2012):

$$\zeta_{connection} = [(N-1) - \lambda_{max}] / (\lambda_{max} - \lambda_1) \quad (3)$$

$$\zeta_{wiring} = 1 - \zeta_{connection} \quad (4)$$

λ_1 is the observed spectral radius.

The sum of the absolute values of the graph spectrum is called graph energy (the name is derived from its origin in physical chemistry):

$$E(g) = \sum |\lambda_i| \quad (5)$$

In the context of this study positive and negative eigenvalues indicate, respectively, divergent and convergent trends. Divergence occurs where the same starting point (e.g., a doline) can lead to multiple pathways or outcomes. Convergent trends occur where multiple starting points can lead to a given outcome. Graph energy thus indicates the overall strength of convergence and divergence present.

The Laplacian matrix of adjacency matrix A is

$$L = D - A, \quad (6)$$

D is the degree matrix, whose diagonal elements are the degree of each node (number of edges incident to that node), with all other elements 0. The largest eigenvalue $\lambda_1(L)$ is called the Laplacian spectral radius, which is inversely related to dynamical stability. For the type of graph of the type considered here the stability condition is

$$h < 2/\lambda_1(L) \quad (7)$$

where h is a time step for network change (Gupta et al. 2003). Thus, as the Laplacian spectral radius increases, smaller time steps are necessary to observe stability.

$\lambda_N[L] = 0$, and the largest nonzero eigenvalue of L , $\lambda_{N-1}[L]$, is called algebraic connectivity ($\alpha[G]$), and is a measure of graph synchronization. Higher $\alpha[G]$ indicates a greater propensity for changes to occur simultaneously or in rapid succession, and vice-versa.

These metrics are described in standard texts on algebraic or spectral graph theory (e.g., Biggs 1994), and their adaptation to geomorphology and interpretation in the context of historical contingency is outlined by Phillips (2013, 2017).

3. Results

3.1. Meander bend evolution and chronosequence

Based on the GIS-based examination of 33 bends and field studies at two, a meander bend evolution scenario was developed. Bend development begins with the initiation of river incision and meander extension. This involves vertical erosion of the river channel and lateral erosion across the interior of developing bend. On the outer bend, slopes are steepened and tributaries truncated, stimulating fluvial incision by tributaries and inhibiting karstification, while on the bend interior, tributaries are deflected toward downstream end of developing bend. As lateral erosion of the slip-off slope continues on the inner bend, exposure of fresh limestone surfaces stimulates dissolution and karst development. Meanwhile, groundwater flow bypasses the developing bend by exploiting

and enlarging joints across the meander. Enlargement of these conduits facilitates collapse dolines on the surface. Enlargement of dolines forms uvalas and autogenic karst valleys. Any joint-guided conduit flow toward the meander apex (as opposed to across the meander) results in formation of karst pocket valleys on lower strath surfaces due to collapse stimulated by a combination of conduit enlargement and surface erosion. More rapid recent incision of the Kentucky River creates a steeper slipoff surface in the lower valley. Here, steeper slopes compared to higher elevation areas of the meander interior are more favorable to mass wasting and less favorable to karstification. Small incised channels may form from pocket valleys or joint-guided slope failures. Throughout, the valley bottom is dominated by Kentucky River fluvial processes. Small incised streams may cross the floodplain, and dolines form as alluvium collapses into karst cavities in underlying limestone.

Six surfaces were recognized at most meanders, including the two examined in detail in the field. The oldest is the upland at the innermost portion not directly affected (eroded) by extension of the bend. Next are three strath terrace surfaces (T1, T2, T3) in order of descending elevation and age. T3 is separated from the modern, active Kentucky River valley bottom by a steep slope. This could perhaps be considered another strath, but is much steeper than the others and is dominated by mass wasting features and rock outcrops and is termed valley side transition (VST). The valley bottom includes the Kentucky River channel, active floodplain, and sometimes a narrow alluvial (as opposed to strath) terrace. These surfaces are shown in Table 1. Figs. 2 and 3 show these surfaces at the two field study sites. The valley bottom was identified based on the low-relief topography adjacent to the river, with a continuous alluvial cover. The VST was delineated based on the steep slope gradient (>0.25). The T1, T2, and T3 surfaces all have rounded quartz gravels on the treads, indicating former channel positions, while the upland lacks these features. Map boundaries in Figs. 1 and 2 are placed at the base of scarps or risers and/or boundaries of exposure of different geological formations.

Of the 19 meanders in the Inner Bluegrass section (see Fig. 1), all but one have evidence of terrace tread-and-riser morphology evident from LiDAR-based topographic maps (Fig. 4). The exception is transgressed by several mapped faults, erosion along which has obscured any clear topographic evidence of terraces. Eighteen of the 19 also show the steep VST zone, and all show exposure of one to three geologic formations between the uppermost Lexington Limestone and the valley-bottom Quaternary alluvium. All are dominated by lithologies



Fig. 2. Polly's Bend study site showing geomorphic surfaces/chronosequence members. Dotted lines indicate approximate boundaries. Base map is shaded relief based on 1.5 m resolution digital elevation model. Area shown is about 2.7 km (north-south) by 2.5 km (east-west). Coordinates at center are 37.8022° N, 84.6472° W.

classified as having high and/or very high karst potential, and all have visible evidence suggesting occurrence of the major landforms described in Section 3.2—though positive identification is not possible in all cases from the GIS data alone.

The mean slope gradient from upland to river (based on a transect normal to the apex) is 0.071 at the Polly's Bend site and 0.056 at Bowman's Bend. This includes gentler slopes on the strath terrace treads (0.004 to 0.010) and steeper slopes on the terrace risers and the valley side transition area. The latter have gradients of 0.251 and 0.381 at the two sites, respectively.

Table 1
Chronosequence members.

Surface	Description	Topographic/morphological indicators	Geological/pedological indicators	Interpretation
Upland	Interior meander bend area with little or no lateral erosion by Kentucky River	More or less accordant hilltops, but strongly dissected or pockmarked by karst features	Lexington Limestone surficial geology; few to no rounded quartz gravels; little or no sand	Limited direct effects of meander development
T1	Oldest, highest strath terrace, farthest from meander apex	Scarp on lower side; discontinuous scarp on upper side, relatively gentle average slope between	Common rounded quartz gravels, sandy soil patches, Chenault soil series common, Tyrone Limestone surficial geology with some Lexington Limestone	Lateral erosion & meander extension associated with relatively slow incision, followed by more rapid incision
T2	Intermediate between T1 and T3	Scarps on upper and lower sides; relatively gentle average slope between	Common rounded quartz gravels, sandy soil patches, Chenault soil series common, Tyrone Limestone surficial geology	Lateral erosion & meander extension associated with relatively slow incision, followed by more rapid incision
T3	Youngest, lowest strath terrace, closest to meander apex	Convex shoulder transition to valley wall slope on lower side; scarp on upper side; relatively gentle average slope between	Common rounded quartz gravels, sandy soil patches, Chenault soil series common, Tyrone Limestone surficial geology with some Camp Nelson Limestone.	Lateral erosion & meander extension associated with relatively slow incision, followed by more rapid incision
Valley wall transition	Steep transitional valley side area between strath terraces and river valley bottom	Steep-to-nearly flat slope inflection on lower side; convex should on upper side; steep linear or weakly convex or concave segments between; slope failure features	Thin residual soils, rock outcrops, cliffs, rare to occasional rounded quartz gravels, Camp Nelson Limestone exposed	Relatively rapid late-glacial & post glacial incision
Valley bottom	Active Kentucky River channel, riparian zone, and floodplain	Active Kentucky River channel & floodplain surfaces; slope inflection at base of valley way	Recent alluvium; floodplain & alluvial terrace soils	Active fluvial processes, & inputs from steep slopes above

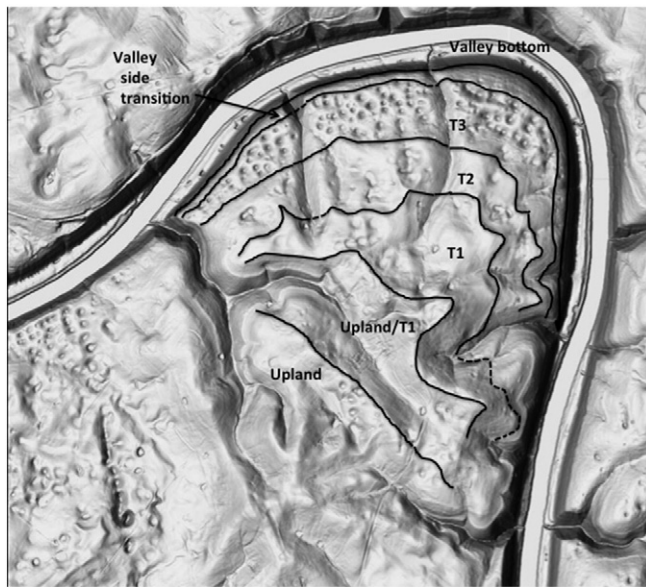


Fig. 3. Bowman's Bend study site showing geomorphic surfaces/chronosequence members. Dotted lines indicate approximate boundaries. Base map is shaded relief based on 1.5 m resolution digital elevation model. Area shown is about 3.2 km (north-south) by 3.5 km (east-west). Coordinates at center are 37.8161° N, 84.6927° W.

3.2. Landforms

The key landforms found indicating karst and fluvial processes are shown in Table 2. Swallets and shafts were detectable only in the field; all the others were visible via GIS data, though some required field verification. Field work at Bowman's and Polly's Bends showed that all features identified via imagery are indeed present and correctly identified. However, some features, particularly smaller dolines, pocket

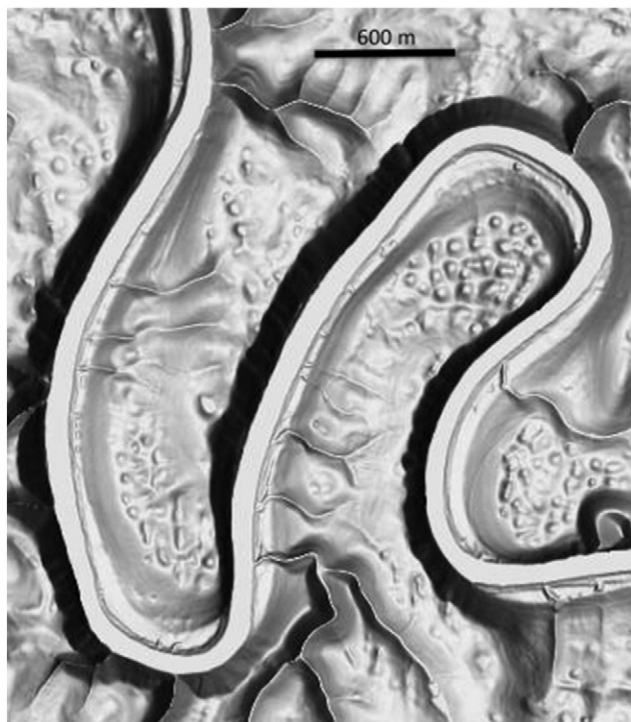


Fig. 4. Shaded relief map of unnamed bends upstream of Frankfort, KY. Coordinates at the midpoint of the image are 37.90° N, 84.79° W.

Table 2
Fluviokarst landforms on Kentucky River meander bend interiors.

Landform	Definition
Doline	Surface depression formed primarily by dissolution; karst sinkhole.
Uvala Karst valley	Larger depression formed by coalescence of dolines. Autogenic (in this case) valley formed primarily by dissolution. May have ephemeral surface channels in valley bottom activated during wet periods when underlying conduits overflow. Swallets and dolines occur in valley bottom.
Pocket valley	Steep valleys formed by collapse or erosional exhumation of cave passages or larger conduits. Characterized by limited surface drainage areas, steep, often amphitheater-like valley heads, exposed bedrock within the valley, and groundwater seepage along joints, bedding planes, and small conduits exposed within the valley
Unincised channel	Fluvial stream channel that is not strongly incised; typically found on upper reaches of tributaries
Incised channel	Strongly incised river or stream channel
Cliff	Subvertical to overhanging slope with exposed bedrock
Alluvial collapse doline	Sinkhole formed by collapse of Kentucky River floodplain deposits into underlying karst cavity or depression.
Swallet	Small (typically <0.1 m ² surface area) dissolutional depression. Often relatively shallow and vertical or near vertical.
Shaft	Similar to swallet, but larger and deeper.

valleys, and channels evident in the field were not detectable (or more commonly, ambiguous) in the GIS data. A count of all landforms was not attempted as the focus was on their occurrence relative to the chronosequence. However, at least a dozen of the larger features (valleys and uvalas) were assessed at each site, along with dozens of dolines. The cliff landform is more or less continuous along the edge of the bends. Some examples are shown in field photographs in Fig. 5 and geomorphic maps in Figs. 6 and 7.

Based on the bend evolution described in Section 3.1, an idealized coincidence table of landform occurrence by surface, and associated graph, was developed (Fig. 8). According to the putative sequence, as vertical and lateral river erosion proceeds, the steep valley side slope transition is formed. Surface features here are primarily cliffs associated with mass wasting, pocket valleys formed as karst conduits are exhumed, and incised channels formed in pocket valleys or by whatever surface runoff occurs on the steep slopes, or by headward extension of any local tributaries. Larger tributaries are assumed to be deflected as described earlier. Behind this advancing front a strath terrace forms, where the opening of new and pre-existing joints facilitates formation of dolines and karst valleys. Pocket valleys may also extend into this surface (corresponding with T3), and T2. As the T2 strath continues to develop, additional features form—uvalas from the growth and merger of dolines, and non-incised channels. On the oldest strath terrace (T1) pocket valleys are presumed to have been converted to karst valleys, and the landforms present are the same as those on the adjacent upland—dolines, uvalas, karst valleys, and unincised channels. The active valley bottom potentially has cliffs descending to river level (though these are uncommon on bend interiors), and pocket valleys and incised channels connected directly to the river. Floodplains often feature alluvial collapse dolines, whereby deposited alluvium has collapsed into underlying karst cavities.

The idealized sequence is based on several key propositions. One is that on the steepest slopes surface runoff and mass movements rather than infiltration and groundwater flow are favored, such that dolines, uvalas and karst valleys are unlikely on the VST (Phillips et al. 2004; Martin 2006). A second is that a considerable amount of time is required for dolines to form and grow large enough to form uvalas and karst valleys. Thus, the model supposes that the latter should not appear on T3, but on the older surfaces. On the upland, T1 and T2 the karst valleys and uvalas are considered inevitable due to the age and karst-prone nature of these areas, and groundwater bypassing of meander bends via



Fig. 5. Examples of landforms in the field at Bowman's Bend. Clockwise, from upper left: Shallow uvala on T1 surface; conduits in the wall of a pocket valley on T2; ephemeral unincised channel crossing T2 and T3; small doline on T3; dry karst valley on T2.

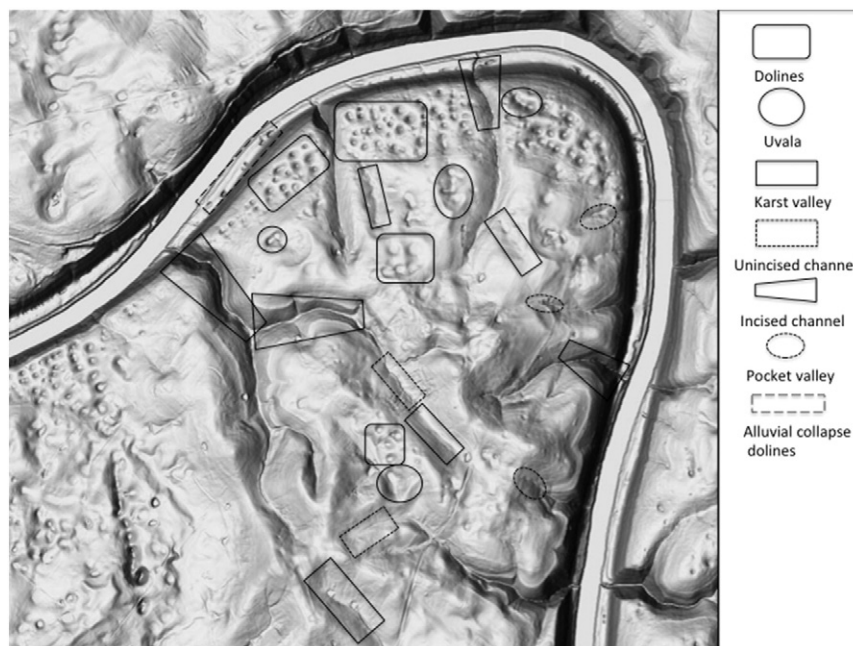


Fig. 6. Examples of landforms mapped at Polly's Bend.



Fig. 7. Examples of landforms mapped at Bowman's Bend.

conduits (Currens et al. 2003; Ray and Blair 2005). Due to the diversion of larger streams away from the apex of the expanding meander and the limited drainage area and thus erosive power of the small local streams (Phillips 2015b), the idealized sequence postulates no incised channels except on the VST, where slopes are sufficient to generate high shear stresses and joint-guided mass movements concentrate surface flow.

In the analyses of landscape evolution below the emphasis is on the upland, strath terraces, and valley side transition, as the valley bottom represents a distinctly different set of dominant processes and environmental controls.

An inventory of the larger landforms (all those in Table 2 except swallets, shafts, and alluvial collapse dolines) by the geomorphic

surfaces was conducted, producing a coincidence table (Table 3) and graphs representing the actual, observed occurrence along the chronosequence (Figs. 9 and 10). The observed coincidence matrix was based on co-occurrence of landform types on each of the five surfaces (upland, T1, T2, T3, VST) at the two field sites. The predicted matrix is based on the predicted coincidence of the landforms on each of the five surfaces as described above.

Table 3

Coincidence matrices. The unshaded numbers indicate the proportion of the surfaces on which the row and column landforms occur together (e.g., dolines and uvalas co-occurred in 7 of 10 cases). The difference table indicates the predicted CI – observed CI.

Observed	Do	Uv	KV	PV	UiC	IC	CI
Doline	1.0	0.7	0.8	0.5	0.5	0.6	0.1
Uvala	0.7	1.0	0.7	0.4	0.4	0.5	0.0
Karst valley	0.8	0.7	1.0	0.5	0.5	0.6	0.1
Pocket valley	0.5	0.4	0.5	1.0	0.2	0.5	0.2
Uncised channel	0.5	0.4	0.5	0.2	1.0	0.2	0.0
Incised channel	0.6	0.5	0.6	0.5	0.2	1.0	0.2
Cliff	0.1	0.0	0.1	0.2	0.0	0.2	1.0
Idealized/predicted	Do	Uv	KV	PV	UiC	IC	CI
Doline	1.0	0.6	0.8	0.4	0.6	0.0	0.0
Uvala	0.6	1.0	0.6	0.2	0.6	0.0	0.0
Karst valley	0.8	0.6	1.0	0.4	0.6	0.0	0.0
Pocket valley	0.4	0.2	0.4	1.0	0.2	0.2	0.2
Uncised channel	0.6	0.6	0.6	0.2	1.0	0.0	0.0
Incised channel	0.0	0.0	0.0	0.2	0.0	1.0	0.2
Cliff	0.0	0.0	0.0	0.2	0.0	0.2	1.0
Difference	Do	Uv	KV	PV	UiC	IC	CI
Doline	0	-0.1	0	-0.1	0.1	-0.6	-0.1
Uvala	-0.1	0	-0.1	-0.2	0.2	-0.5	0
Karst valley	0	-0.1	0	-0.1	0.1	-0.6	-0.1
Pocket valley	-0.1	-0.2	-0.1	0	0	-0.3	0
Uncised channel	0.1	0.2	0.1	0	0	-0.2	0
Incised channel	-0.6	-0.5	-0.6	-0.3	-0.2	0	0
Cliff	-0.1	0	-0.1	0	0	0	0

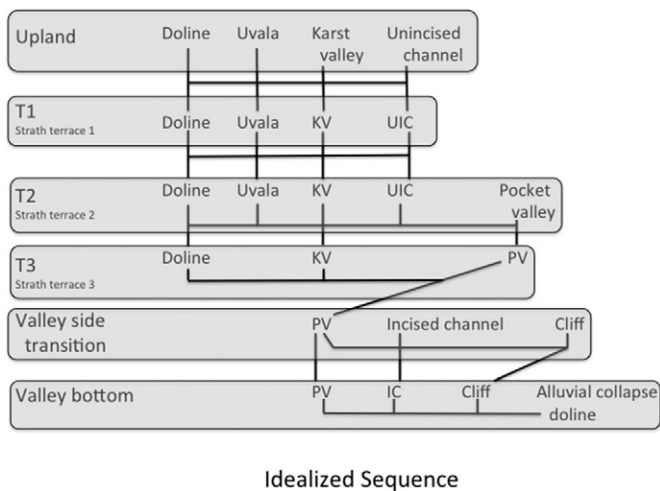
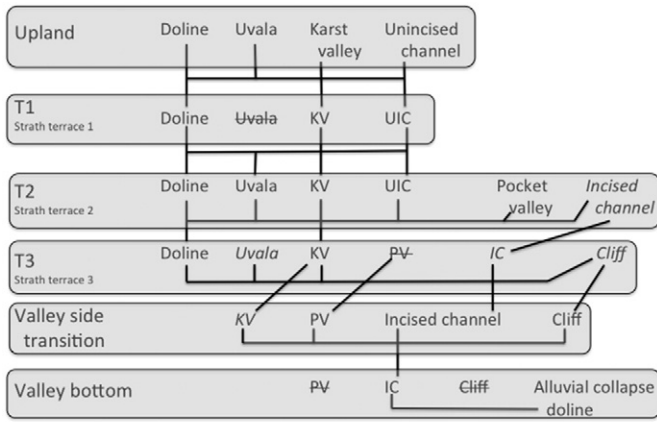


Fig. 8. Graph of predicted or idealized landform occurrence by chronosequence components. The valley bottom is not included in the analyses, but is shown here for completeness.



Polly's Bend

Fig. 9. Graph of observed landform occurrence by chronosequence components at Polly's Bend. The valley bottom is not included in the analyses, but is shown here for completeness. *Italicized* landforms were not included on the indicated surface in the idealized model, but were found in the field. Landforms with strikethroughs were predicted in the idealized model but not observed.

The graphs contain $N = \sum n_q$ nodes, where q ($= 5$ in this case) chronosequence stages or surfaces occur and n_q is the number of landform types at each stage. All nodes (landforms) at each stage are considered to be linked. If the same landform occurs on spatially and temporally adjacent surfaces, they are also considered to be linked.

3.3. Graph analysis

Graph spectral properties were determined for the graphs shown in Figs. 8–10. As a benchmark, they were also computed for a no-historical-contingency case. The latter is based on all seven included landforms occurring on all five surfaces, except for cliffs only on the VST, with links or edges established as described for the other cases. Results are shown in Table 4.

Both observed cases have more nodes and edges than the hypothesized sequence, and higher complexity, as indicated by the spectral radius. $\zeta_{\text{connection}}$ is about 0.7 for all cases, indicating that about 70% of the reduction in complexity compared to a fully-connected (every

node linked to every other) graph of the same N is due to having fewer than the maximum number of edges, and about 30% to the specific pattern of edges (wiring). Both sites had higher graph energy and Laplacian spectral radius than the idealized case, indicating greater instability and more intense divergence and convergence. Algebraic connectivity was higher than the idealized case, indicating a lesser degree of historical contingency. The benchmark case, as expected, has a greater spectral radius, graph energy, Laplacian spectral radius and algebraic connectivity than the other graphs. Geomorphic interpretation of these results is discussed below.

4. Discussion and interpretations

4.1. Landscape evolution

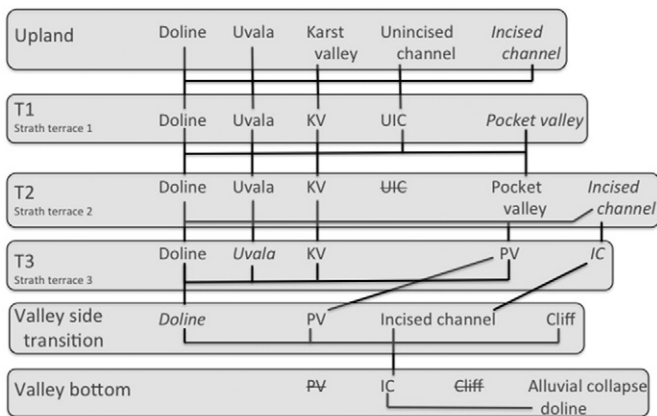
The interior meander bends of the Kentucky River gorge provide a space-for-time substitution opportunity to assess fluviokarst landscape evolution. While this gives some insight and lessons for fluviokarst development in general, we must bear in mind that the Kentucky River/ Inner Bluegrass region (like any landscape) has a unique combination of environmental controls and history. Further, evolution in the bend interiors differs from that of areas adjacent to outer meander bends, or other settings in the region.

As the Kentucky River incises, this steepens valley side slopes. Slope failures and erosion expose bedrock and joints, allowing dolines to open. Local joint-guided streams and pocket valleys dissect the slope. On bend interiors, as the slope flattens behind the advancing meander, cross-bend conduit flow and enlargement occurs, and dense doline concentrations develop. Over time, dolines enlarge and coalesce, forming uvalas and karst valleys. Surface erosion and deposition and valley slope development along streams and pocket valleys also smooth pockmarked topography. If any larger tributaries existed prior to the Quaternary downcutting, they are deflected downstream (relative to the river) from the bend interiors (as discussed by Phillips 2015b). All the while, landform scale transitions among karst and fluvial forms are possible, and facilitated by the falling base level of the river (Phillips 2017). Note that incision has apparently slowed in the last 100 yr. In the early twentieth century a series of navigation locks and dams were constructed on the Kentucky River. Locks are no longer operable except on the lower reaches of the river (beyond the study area), but the low-head dams remain, and the river is essentially a series of long pools and short riffles, slowing channel erosion.

The presence of the three strath terraces implies relative vertical stability for periods since the Quaternary downcutting began. These are possibly associated with episodes where the lower Kentucky River was blocked by slugs of fluvio-glacial outwash moving down the Ohio River, creating lacustrine conditions near the river mouth. This is known to have occurred several times in the late Quaternary, as indicated by lacustrine deposits in the lower Kentucky River valley, as well as those of other Ohio River tributaries in the region (Ray 1974; Andrews 2004; Phillips 2010). The valley side transition zone, which is longer and has greater relief than the terrace risers, suggests a longer period of uninterrupted incision. This is speculative and requires further research to confirm, however. An alternative explanation for episodic bedrock strath terrace formation is based on upstream propagation of knickpoints (Finnegan and Dietrich 2011). However, the latter mechanism is based on cutoffs of incised meanders, the closest of which is >65 km downstream from Bowman's Bend.

4.2. Landform coincidence

The pattern of landform coincidence along the chronosequence indicates more occurrences of incised channels and karst valleys than expected based on the idealized or predicted sequence. The latter was based on the idea that, as larger tributaries are deflected away from the bend interior, only the lower reaches of local tributaries on the



Bowman's Bend

Fig. 10. Graph of observed landform occurrence by chronosequence components at Bowman's Bend. The valley bottom is not included in the analyses, but is shown here for completeness. *Italicized* landforms were not included on the indicated surface in the idealized model, but were found in the field. Landforms with strikethroughs were predicted in the idealized model but not observed.

Table 4
Graph properties.

	N	m	Spectral radius	$\zeta_{\text{connection}}$	ζ_{wiring}	Graph energy	Laplacian spectral radius	Algebraic connectivity
Idealized sequence	19	40	4.845	0.707	0.293	31.677	7.900	0.207
No historical contingency	31	99	6.877	0.699	0.301	59.369	9.683	0.359
Polly's Bend	23	60	6.424	0.725	0.275	40.447	9.583	0.310
Bowman's Bend	24	62	5.470	0.690	0.310	49.952	8.541	0.318

valley side transition (and across the floodplain) would be incised. In fact, incised channels occur on all surfaces except T1 at Bowman's Bend, and on T2 and T3 at Polly's Bend. These appear to be associated with capture of both surface and groundwater flow by pocket valleys, converting them to fluvial channels.

The negative values in the difference section of Table 3 indicate a higher observed coincidence than expected or predicted. The off-diagonal entries indicate seven cases where the observed and predicted were identical, 11 with negative values, and only three with positive values (fewer observed than predicted coincidences). This mainly reflects persistence of features as terraces age that was not predicted. The positive values indicate features that were expected but not observed (unincised channels).

$CI \geq 0.7$ —all associated with coincidence of dolines, uvalas, and karst valleys—are seen as representing the genetic relationships among the formations of these features, along with the ubiquity of dolines.

4.3. Graph properties

The no-historical-contingency (NHC) benchmark is founded on the hypothetical situation where a given set of landforms occurs throughout the chronosequence, with no additions or deletions as the bends evolve except cliffs in the VST zone. The higher spectral radius and Laplacian spectral radius for the NHC case indicate greater complexity and instability, indicating that historical contingency reduces complexity by limiting some developmental pathways. However, these limitations are less in the observed cases than for the idealized sequence. The relatively consistent ζ values for all graphs suggests that the reduction in complexity observed is inherent to the basic structure (all landforms connected to all others within a chronosequence member, and to similar landforms on adjacent members).

Graph energy is the sum of the absolute values of all the graph eigenvalues. Positive eigenvalues represent divergent trends, where the same starting point (e.g., a doline) can lead to multiple pathways or outcomes. Negative eigenvalues are associated with convergent trends, where multiple starting points can lead to a given outcome (e.g., a karst valley or incised channel). Graph energy is maximum for the NHC benchmark, and lowest for the idealized chronosequence. The intermediate values

for the study sites are consistent with the notion of greater complexity than the proposed sequence, with more divergence and convergence.

The algebraic connectivity indicates lower inferential synchronization and more historical contingency for the observed patterns than for the NHC case, but the values are much higher than in the hypothesized chronosequence.

Table 5 summarizes differences between observations at the field sites and the hypothesized sequence. The proposed explanations have all been observed in the field in a least one case. With but one exception, these proposed explanations are associated with fluvial-to-karst or karst-to-fluvial landform transitions, or more rapid formation of features than envisioned. Thus the differences between the graph properties of the observed and idealized sequences can be linked to relatively rapid landscape evolution and landform transitions.

4.4. Canalization and mutual reinforcement

Some irreversibility and evolutionary lock-in certainly occurs in the study area. The carbonate lithology with abundant joints and humid climate predisposes the landscape to dissolution and karstification. Widening of joints and enlargement of conduits is irreversible, though some (reversible) plugging by deposited sediment may occur. Once conduits and subsurface cavities are formed, some surface collapse is inevitable. Locally steep topographic gradients associated with dolines, etc., combined with the humid climate and thin, clayey soils dictates that some surface runoff is inevitable, leading to modification of surface topography by runoff and fluvial processes.

However, canalization is not particularly strong, as indicated by the low levels of historical contingency relative to the hypothesized ideal sequence. Deviations from the idealized chronosequence are primarily due to landform transitions that allow karst-to-fluvial (and vice versa) conversions to occur rather than canalization along a karst or fluvial pathway. These landform transitions also lead to the high levels of graph complexity observed at the study sites, with the spectral radius and Laplacian spectral radius, particularly at Polly's Bend, approaching the values of the no-historical-contingency benchmark.

The fact that the incision of the Kentucky River provides (over the last ca. 1.5 Ma) a steadily lowering base level for both fluvial and karst

Table 5
Observed deviations from hypothesized chronosequences. Highlighted potential explanations have been observed in at least one case in the field. BB = Bowman's Bend; PB = Polly's Bend.

Hypothesized	Basis	Observed	Possible explanations
No dolines or karst valleys on VST	Steep slopes discourage development of these features	Dolines at BB; karst valley at PB	Exposed shaft or swallet develops collapse doline; karst capture of fluvial channel to form karst valley
No uvalas or karst valleys on T3	Insufficient time for doline growth & coalescence or conversion of pocket valleys to karst valleys	Uvalas & pocket valleys at BB & PB	Growth & coalescence more rapid than expected; karst capture of fluvial channel to form karst valley
Uvalas present on upland, T1, T2	Inevitable doline growth & coalescence with sufficient time	No uvalas on T1 at PB	Small preserved area of T1 at PB
No incised channels except on VST	Incision possible only in valley bottom alluvium or lower reaches of local streams on VST	Incised channels on upland at BB, & on T2, T3 at both sites	Incision of deflected tributary at BB, conversion of pocket valleys to incised channels
Unincised channels on upland, T1, T2	Fluvial channels present but insufficient time & discharge to produce incision	No unincised channels on T2 at BB	Stream power sufficient to drive incision; conversion of pocket valleys to incised channels; karst capture of fluvial channel to form karst valley

processes maintains active denudation by both dissolutional and mechanical, and surface and subsurface processes. The potential for landforms to be autogenically modified both within and between fluvial landforms (incised and unincised channels) and karst features (dolines, unvalas, karst valleys, pocket valleys) suggests that, at least at the scale of individual landforms, mutual reinforcement of karst and fluvial processes rather than canalization is the rule on the studied chronosequences. Phillips (2017) came to a similar conclusion based on the study of specific features that indicate recent or ongoing fluvial-to-karst or karst-to-fluvial transitions.

5. Conclusions

The evolution of meander bends in the Kentucky River gorge area over the past ~1.5 Ma has created a series strath terraces that represent a chronosequence from the youngest valley side transition zone near the valley bottom to the oldest upland (not laterally eroded) surface. This five-part chronosequence was analyzed in terms of the landforms that occur at each stage or surface. Landform coincidence analysis shows higher coincidence indices than would be expected based on an idealized chronosequence, representing genetic relationships (common causality) among some features and possibly unanticipated persistence of some features on older surfaces.

An analysis of a graph (network) based representation of the chronosequence shows that observations at two study sites produce graphs more complex and with less historical contingency than the idealized sequence. Indeed, some of the spectral graph measures for the field sites more closely approximate a purely hypothetical no-historical-contingency benchmark graph. The deviations of observation from the idealized expectations, and the high levels of graph complexity both point to potential transitions among landform types rather than canalization along a particular evolutionary pathway as being the dominant phenomenon. As the base level of both the fluvial and karst landforms is lowered as the meanders expand, both fluvial and karst denudation are rejuvenated, and landform transitions remain active.

Acknowledgements

The constructive criticism of an anonymous reviewer greatly improved the final version of this paper.

References

- Andrews Jr., W.M., 2004. Geologic Controls on Plio-Pleistocene Drainage Evolution of the Kentucky River in Central Kentucky. University of Kentucky, Lexington, PhD dissertation.
- Bahtijarevic, A., Faivre, S., 2016. Quantitative comparative geomorphological analysis of fluvial and karst relief of Florida. *Environ. Earth Sci.* 75 article no. 428. (doi: 10.1007/s12665-016-5397-8).
- Benac, C., Juracic, M., Maticec, D., Ruzic, I., Pikelj, K., 2013. Fluviokarst and classical karst: examples from the Dinarics (Krk Island, northern Adriatic, Croatia). *Geomorphology* 184, 64–73.
- Berlow, E.L., 1997. From canalization to contingency: historical effects in a successional rocky intertidal community. *Ecol. Monogr.* 67, 435–460.
- Beven, K., 2015. What we see now: event-persistence and the predictability of hydro-eco-geomorphological systems. *Ecol. Model.* 298, 4–15.
- Biber, P., Seifert, S., Zaplata, M.K., Schaaf, W., Pretzsch, H., Fischer, A., 2013. Relationships between substrate, surface characteristics, and vegetation in an initial ecosystem. *Biogeosciences* 10, 8283–8303.
- Biggs, N., 1994. Algebraic Graph Theory. 2nd ed. Cambridge University Press.
- Bocic, N., Pahernik, M., Mihevic, A., 2015. Geomorphological significance of the palaeodrainage network on a karst plateau: the Una-Korana plateau, Dinaric karst, Croatia. *Geomorphology* 247, 55–65.
- Caloi, P., 1964. On the canalization of seismic energy. *Ann. Geophys.* 17, 513–522.
- Cressman, E.R., Hrabar, S.V., 1970. Geologic Map of the Wilmore Quadrangle, Central Kentucky. U.S. Geological Survey 1:24,000 map sheet, Washington.
- Currens, J.C., Paylor, R.L., Ray, J.A., 2003. Mapped Karst Groundwater Basins in the Harrodsburg 30 × 60 Minute Quadrangle (1:100,000 scale map). Kentucky Geological Survey. <https://www.uky.edu/KGS/water/research/kaatlas.htm>.
- Cvijic, J., 1918. L'hydrographie souterraine et l'évolution morphologique du karst. *Revue de Géographie Alpine* 6, 375–426.
- Dury, G.H., 1964. Principles of underfit streams. U.S. Geological Survey Professional Paper 452-A (67 p).
- Finnegan, N.J., Dietrich, W.E., 2011. Episodic bedrock strath terrace formation due to meander migration and cutoff. *Geology* 39, 143–146.
- Ford, D., 2007. Jovan Cvijic and the founding of karst geomorphology. *Environ. Geol.* 51, 675–684.
- Gupta, V., Hasibi, B., Murray, R.M., 2003. Stability analysis of stochastically varying formations of dynamic agents. Proceedings of the 42nd IEE Conference of Decision and Control 1, pp. 504–509.
- Jaillet, S., Pons-Branchu, E., Brulhet, J., Hamelin, B., 2004. Karstification as geomorphological evidence of river incision: the karst of Cousance and the Marne valley (eastern Paris Basin). *Terra Nova* 16, 167–172.
- Jerin, T., Phillips, J.D., 2017. Local efficiency in fluvial systems: lessons from icicle bend. *Geomorphology* 282, 119–130.
- Kauffman, G., 2009. Modelling karst geomorphology on different time scales. *Geomorphology* 106, 62–77.
- Levchenko, V.F., Starobogatov, Y.I., 1997. Ecological crises as ordinary evolutionary events canalised by the biosphere. *International Journal of Computing Anticipatory Systems* 1, 105–117.
- Lipar, M., Ferk, M., 2015. Karst pocket valleys and their implications on Pliocene-Quaternary hydrology and climate: examples from Nullarbor Plain, southern Australia. *Earth Sci. Rev.* 150, 1–13.
- Martin, L.L., 2006. Effects of Forest and Grass Vegetation on Fluviokarst Hillslope Hydrology, Bowman's Bend. PhD dissertation, University of Kentucky, Lexington, Kentucky.
- Maurer, T., Gerke, H.H., 2016. Processes and modeling of initial soil and landscape development: a review. *Vadose Zone J.* 15 (doi:10.2136/vzj2016.05.0048).
- Naylor, L., Stephenson, W., 2010. On the role of discontinuities in mediating shore platform erosion. *Geomorphology* 114, 89–100.
- Ortega Becerril, J.A., Heydt, G.G., Duran, J.J., 2010. The role of sculpted forms and endokarstic active conduits in the development of fluviokarstic canyons. The Rio Puro cave conduit (Spain). In: Andreo, B. (Ed.), *Advances in Research in Karst Media*. Springer, Berlin, pp. 387–392.
- Perron, T., Fagherazzi, S., 2012. The legacy of initial conditions in landscape evolution. *Earth Surf. Process. Landf.* 37, 52–63.
- Phillips, J.D., 2010. Amplifiers, filters, and the response of Kentucky rivers to climate change. *Clim. Chang.* 10, 571–595.
- Phillips, J.D., 2012. Synchronization and scale in geomorphic systems. *Geomorphology* 137, 150–158.
- Phillips, J.D., 2013. Networks of historical contingency in earth surface systems. *J. Geol.* 121, 1–16.
- Phillips, J.D., 2015a. The robustness of chronosequences. *Ecol. Model.* 298, 16–23.
- Phillips, J.D., 2015b. Badass geomorphology. *Earth Surf. Process. Landf.* 40, 22–33.
- Phillips, J.D., 2016. Complexity of earth surface system evolutionary pathways. *Math. Geosci.* 48, 743–765.
- Phillips, J.D., 2017. Landform transitions in a fluviokarst landscape. *Z. Geomorphol.* 61 (2), 109–122.
- Phillips, J.D., Lutz, J.D., 2008. Profile convexities in bedrock and alluvial streams. *Geomorphology* 102, 554–566.
- Phillips, J.D., Walls, M.D., 2004. Flow partitioning and unstable divergence in fluviokarst evolution in central Kentucky. *Nonlinear Process. Geophys.* 11, 371–381.
- Phillips, J.D., Martin, L.L., Nordberg, V.G., Andrews, W., 2004. Divergent evolution in fluviokarst landscapes of central Kentucky. *Earth Surf. Process. Landf.* 29, 799–819.
- Raab, T., Krummelbein, J., Schneider, A., Gerwin, W., Maurer, T., Naeth, M.A., 2012. Initial ecosystem processes as key factors of landscape development—a review. *Phys. Geogr.* 33, 305–343.
- Ray, L.L., 1974. Geomorphology and Quaternary geology of the Glaciated Ohio River Valley; a Reconnaissance Study. U.S. Geological Survey Professional Paper PP-826 (77 p).
- Ray, J.A., Blair, R.J., 2005. Large perennial springs of Kentucky: their identification, base flow, catchment, and classification. In: Beck, B.F. (Ed.), *Sinkholes and the Engineering and Environmental Impacts of Karst*. Geotechnical Special Publication 144, American Society of Civil Engineers, pp. 410–422.
- Roglic, J., 1964. Karst valleys in the Dinaric karst. *Erdkunde* 18, 113–116.
- Šamonil, P., Antolík, L., Svoboda, M., Adam, D., 2009. Dynamics of windthrow events in a natural fir-beech forest in the Carpathian mountains. *For. Ecol. Manag.* 257, 1148–1156.
- Šamonil, P., Schaetzl, R.J., Valtera, M., Goliáš, V., Baldrian, P., Vašíčková, I., Adam, D., Janík, D., Hort, L., 2013. Crossdating of disturbances by tree uprooting: can treethrow microtopography persist for 6,000 years? *For. Ecol. Manag.* 307, 123–135.
- Šamonil, P., Vašíčková, I., Daněk, P., Janík, D., Adam, D., 2014. Disturbances can control fine-scale pedodiversity in old-growth forests: is the soil evolution theory disturbed as well? *Biogeosciences* 11, 5889–5905.
- Sauro, U., 2002. The Monti Berici: a peculiar type of karst in the southern alps. *Acta Carsologica* 31, 99–114.
- Sawicki, L.R., 1909. Ein Beitrag zum geographischen Zyklus im Karst. *Geogr. Z.* 15 (185–204), 259–281.
- Sommer, M., Gerke, H.H., Deumlich, D., 2008. Modelling soil landscape genesis—a time split approach for hummocky agricultural landscapes. *Geoderma* 145, 480–493.
- Stallins, J.A., 2006. Geomorphology and ecology: unifying themes for complex systems in biogeomorphology. *Geomorphology* 77, 207–216.
- Teller, J.T., Goldthwait, R.P., 1991. The old Kentucky River; a major tributary to the Teays River. *Geol. Soc. Am. Spec. Pap.* 258, 29–42.
- Thraillkill, J., Sullivan, S.B., Gouzie, D.R., 1991. Flow parameters in a shallow conduit-flow carbonate aquifer, inner bluegrass karst region, Kentucky, USA. *J. Hydrol.* 129, 87–108.
- Tiria, L., Vijulie, I., 2013. Structural-tectonic controls and geomorphology of the karst corridors in alpine limestone ridges, southern Carpathians, Romania. *Geomorphology* 197, 123–136.
- Twidale, C.R., 1991. A model of landscape evolution involving increased and increasing relief amplitude. *Z. Geomorphol.* 35, 85–109.

- Vercruyse, K., Grabowski, R.C., Rickson, R.J., 2017. Suspended sediment transport dynamics in rivers: multi-scale drivers of temporal variation. *Earth Sci. Rev.* 166, 38–52.
- Verleysdonk, S., Krautblatter, M., 2011. Sensitivity and path dependence of mountain permafrost systems. *Geografiska Annaler Series A* 93, 113–135.
- Waddington, C.H., 1942. Canalization of development and the inheritance of acquired characteristics. *Nature* 150, 563–565.
- Wainwright, J., Turnbull, L., Ibrahim, T.G., Lexartza-Artza, I., Thornton, S.F., Brazier, R.E., 2011. Linking environmental régimes, space and time: interpretations of structural and functional connectivity. *Geomorphology* 126, 387–404.
- White, W.B., 2009. The evolution of Appalachian fluviokarst: competition between stream erosion, cave development, surface denudation and tectonic uplift. *Journal of Cave and Karst Studies* 71, 159–167.
- Woodside, J., Peterson, Dogwiler T., 2015. Longitudinal profile and sediment mobility as geomorphic tools to interpret the history of a fluviokarst stream system. *Int. J. Speleol.* 44, 197–206.